Journal of Scientific & Industrial Research
Vol. 79, April 2020, pp. 306–311

Control Implementation of Squirrel Cage Induction Generator based Wind Energy Conversion System

Arika Singh[1], Hemant Ahuja[2*], Vikas Bhadoria[2] and Sachin Singh[3]

[1]Department of Electrical Engineering, Krishna Institute of Engineering and Technology, Ghaziabad, Uttar Pradesh, India

[2]Department of Electrical Engineering, ABES Engineering College, Ghaziabad, Uttar Pradesh, India

[3]Department of Electrical Engineering, Institute of Engineering and Technology, Lucknow, Uttar Pradesh, India

Received 3 April 2019; revised 7 November 2019; accepted 27 February 2020

Trends towards PC-based computing platforms have given a path to innovate advanced, model-based control algorithms for the control of wind energy conversion systems. These advanced models allow us to gain increased reliability and improved efficiency. This work is focused on the digital signal processor based implementation aspects of a variable speed, grid connected; squirrel cage induction generator based wind energy conversion systems. Control design using a voltage source converter at the machine side have been described, designed, modeled and analyzed. A comprehensive analysis of the designed system is performed in terms of the active power harnessed, power quality and reactive power control. Optimal power point operation has been implemented so that highest available power is harnessed for varying wind velocities. A 2.2kW prototype with back to back connected voltage source converter has been implemented in hardware using TMS320F2812 digital signal processor. The experimental results illustrate the excellent performance of the system.

Keywords: SCIG, Vector Control, Voltage source converters, WECS, DSP

Introduction

Wind energy conversion systems (WECS) using squirrel cage induction generator (SCIG) are becoming popular nowadays due to qualities like ruggedness in harsh environments, low cost and easy availability.[1,2] Different control designs for WECS, discussed in literature, claims that an insulated-gate bipolar transistor (IGBT) based Pulse Width Modulation (PWM) Voltage Source Converter provides an effective control over the power factor at the grid interface, active and reactive power and provides good efficiency.[3–5] The state of the art WECS, based on various generator and converter combinations is presented by Bose *et al*.[6] As an add-on to literature, this paper intends to provide the performance analysis and hardware implementation of an SCIG based WECS. The paper is structured to provide the prototype description including WT emulation, grid connection and software requirements followed by MSC and GSC control, Results, and conclusion.

Prototype Description and Control Implementation

Two configurations could have been used for developing the prototype; one is by using a boost converter and the second is with the use of VSCs for the grid integration of WECS. It has been observed through literature that the dynamic response of a back to back VSC based WECS is better than the boost converter[6], therefore a prototype based on VSCs is developed in the proposed work. The schematic diagram of the overall system is shown in Fig. 1. A DC shunt motor, emulating wind turbine (WT) characteristics, operate as the prime mover for the SCIG. GSC is connected to the grid through a filter inductance and a transformer. The transformer is used to step up the voltage output of the generator to match the grid voltage. It also isolates the controller from the power grid. TMS320F2812 digital signal processor (DSP) controls the pulse generation for the power converters. It is programmed using a PC through parallel port/JTAG interface. MSC is controlled to harness maximum power from the WECS for a given wind velocity and GSC is controlled to obtain constant DC link voltage. The DC motor coupled to the SCIG act as the prime mover. Wind velocity variations are emulated by varying the speed of the shunt motor by either armature voltage control or by field control.

Optimal Power Control and Wind Turbine Emulation

The WT is emulated by a DC motor drive having torque control. The power extracted (P_{wt}) by a wind turbine is

*Author for Correspondence
E-mail: ahuja.iitd@gmail.com

$$P_{wt} = 0.5\, C_p\,(\lambda, \beta)\, \rho\, A\, v^3 \quad \ldots (1)$$

Where ρ, A *and* v represents the air density, swept area of the WT blades and the wind speed respectively. C_p represents the power extraction efficiency or the wind power coefficient which is a function of 'β', the pitch angle and 'λ', the tip speed ratio. The tip speed ratio is given as $R*\omega_l / v$, where R is radius of the wind turbine and ω_l is the shaft speed. The power harnessed by the WT is highly dependent upon tip speed ratio when β is unchanged.[7] There is a well determined, maximum power conversion efficiency $C_{p,max}$ for a specific value of 'λ'. The optimal power control can be achieved without difficulty, if λ is controlled to accomplish the $C_{p,max}$ for a particular wind speed. From equation (1) and the expression, $\lambda = R*\omega_l / v$, it follows that

$$P_{wt} = 0.5\, C_p(\lambda, \beta)\, \pi\, R^2\, v^3\, \rho = 0.5\, \{C_p(\lambda) / \lambda^3\}\, \pi\, R^5\, \omega_l^3\, \rho \quad \ldots (2)$$

The corresponding torque equation is given as

$$T_{wt} = K\, \omega_l^2 \quad \ldots (3)$$

Where $K = 0.5\, \{C_p(\lambda) / \lambda^3\}\, \pi\, R^5\, \rho \quad \ldots (4)$

Power Signal feedback (PSF) control is implemented in this work, by using the maximum power curves of the WT i.e. by keeping the value of 'λ' at λ_{opt} for a given wind velocity. $C_p(\lambda)$ can also be fixed at $C_{p,max}$ and thus maximum power can be extracted from the WT.[8] Here, the optimum value of λ is maintained at $\lambda_{opt} = 8.1$ and $C_p(\lambda_{opt})$ is computed as 0.47. The WT gives its rated power at the base wind speed of 10m/s.

The torque of WT is controlled in the actual hardware set up by controlling the DC motor torque T_{DC}.

$$T_{wt} = T_{DC} = K_t\, \phi\, I_a \quad \ldots (5)$$

where, ϕ is the field flux and I_a is the armature current of DC machine. The mechanical dynamics of the turbine and generator is given by

$$T_{wt} - T_{gen} \approx J\, (d\omega_m / d_t) \quad \ldots (6)$$

where T_{gen} is the counter torque developed by the generator including friction. The system reaches a steady operating condition when the two torques balance each other.

SCIG and Grid Connection

The SCIG used is a three-phase, 2.2kW, 415 V, 50 Hz, 4-pole, delta connected machine. The equivalent circuit parameters obtained through laboratory tests are, respectively, R_c = 1661Ω, R_1 = 3.06 Ω, R_2 = 4.65Ω, L_m = 0.247135 H and L_{l1} = L_{l2} = 0.0143239 H. Two10 kVA, Semikron make, three phase IGBT converter stacks are used as MSC and GSC. The maximum switching frequency of the converter is 15 kHz and the IGBT Driver used is SKHI22B with 5V gate pulses. DC Link Capacitance is 1650μF with max 750V DC Capacity, a peak current rating of 30 A and continuous current rating of 14 A at15 kHz.

Power Converter Control and Software Requirements

Spectrum Digital eZdspF2818 kit powered by Texas Instruments TMS320F2812 DSP processor has been used for hardware implementation. This DSP is a powerful 150MHz processor generally used for machine control applications. It has 12 complementary PWM outputs divided into two groups each having 6 outputs. In addition it has 4 independent PWM channels totaling to 16 PWM outputs. Also, it has 16 ADC channels. An opto-coupler IC 6N136 is used for providing isolation between the power and control modules. The common emitter amplifier at the output of the opto-coupler provides required voltage and current amplification for the gating pulses to trigger the IGBTs in the MSC and GSC. Hall Effect voltage sensors are used to sense phase voltages of the grid and the DC link voltage and also for speed measurement. Since ADC channels input voltage is 0 – 3V only, careful amplification or attenuation and level shifting of the measured AC quantities have to be performed before connecting them to the ADC channels. MATLAB Simulink with Target Support Package, Real-time Workshop and HDL Coder toolboxes allows code generation for Texas Instruments C2000 series processors. Model is made in simulink and the corresponding C code is generated using Real-time workshop with help of C compiler provided by the visual studio. This code is downloaded to the processor through the Integrated Development Environment (IDE) provided by Code Composer Studio (CCS). The PC interface used is a parallel port connection with JTAG capabilities. TMS320F2812 being a fixed point processor, all calculations have to be performed in fixed point data type. The special IQ – Math library provided by the

Target support package enables calculations in fixed point data type.

Control Strategy for MSC

The control structures for WECS are largely classified on the basis of the power electronic converters /topology used at the machine as well as at the grid side and its associated control. These converters are responsible to achieve optimal power point operation throughout, provide variable speed control and supply the required reactive power to the squirrel cage generator. The following section provides the engineering and control design for SCIG with PWM converter as the MSC. The GSC control is discussed in the later section. The block diagram of a grid connected system with a PWM converter at the machine side and the grid side is already shown in Fig. 1. A capacitor bank, which is required to provide reactive power to the induction generator for establishing the air gap flux, is eliminated in this configuration as PWM converter provides the reactive power support but at an increased converter rating. The DC link capacitor act as a temporary energy storage element. The action of GSC is to keep the DC link voltage constant and inject the generated power to the grid satisfying all the grid connection requirements. With a VSC employed at the machine side, the generator speed becomes controllable and MPPT can be easily achieved. Either of the vector control or the direct torque control is applied to this VSC to achieve an efficient and controlled variable speed operation[9]. The current drawn is very near to sinusoidal and so is the reason, the power devices and the generator face reduced stress. Losses are also considerably reduced. It also helps in achieving good voltage regulation. The magnetizing current could also be controlled, thereby improving the efficiency of the generator by reducing the losses. In this work, rotor flux oriented vector control is adopted for controlling the generator. The Electromechanical torque produced and the flux can be written as:

$$T_e = \frac{3}{2} P \frac{L_m}{L_r} \psi_{rd} i_{sq} = \frac{3}{2} P \frac{L_m^2}{L_r} i_{sd} i_{sq} \quad \ldots (7)$$

$$|\bar{\psi}_{r\psi r}| = \psi_{rd} = L_m |\bar{i}_{mr}| = L_m i_{sd} \quad \ldots (8)$$

It could be seen from (7) and (8) that a decoupled control of torque and flux is feasible by controlling the corresponding current components, and this forms the basis for vector control. i_{sd} controls the air gap flux and i_{sq} controls the electromagnetic torque. The rotor flux oriented control can be implemented either using a current source inverter or current controlled voltage source inverter (CC-VSI). The latter is employed in this work with a fast current control strategy. The controller schematic is illustrated in Fig. 1. The torque controller dictates the q-axis reference current while the flux controller decides the reference current for d-axis. The rotor flux angle (ρ_r), required for converting the d and q axes currents to three phase currents is estimated by the flux model.

Control of the Grid Side Converter

The main function of the GSC is to control the active power injected to the grid such that a constant DC-link voltage is maintained. Also, the GSC controls the reactive power transfer between the converter and the grid, to ensure acceptable power quality at the grid interconnection point. Here, the GSC is operated at unity power factor so that it can work with a minimum rating corresponding to its real power only. The expressions for active and reactive power are given as:

$$P = 1.5 (V_d I_d + V_q I_q) = 1.5 V_d I_d \quad \ldots (9)$$

$$Q = 1.5(-V_d I_q + V_q I_d) = - 1.5 V_d I_q \quad \ldots (10)$$

where, V_d, V_q, I_d and I_q are, respectively, the d and q axes voltage and current delivered to the grid. Aligning the d-axis of the reference frame along the stator voltage phasor, V_q becomes zero. Since the supply voltage is a constant, V_d is a fixed value. So, the active and reactive power will be proportional to I_d and I_q, respectively. The control schematic for the GSC is also presented in Fig. 1. The active and reactive power control is done through the control of I_d and I_q respectively. The reactive power reference is set to zero to maintain the power factor at one. For active power control, the DC link voltage is compared to a reference value and the error is passed through a PI controller to set the d-axis current reference, I_d^*, as illustrated in Fig. 1. Any imbalance in the active power will cause fluctuations in the DC link voltage. The inner current control loop regulated the d-axis current. A similar control strategy consisting of two cascaded loops is used to control the reactive power as well. The outer loop creates the reference for the reactive current, I_q^* from the difference between the required and measured reactive power values. The inner loop regulates the q-axis current. The current

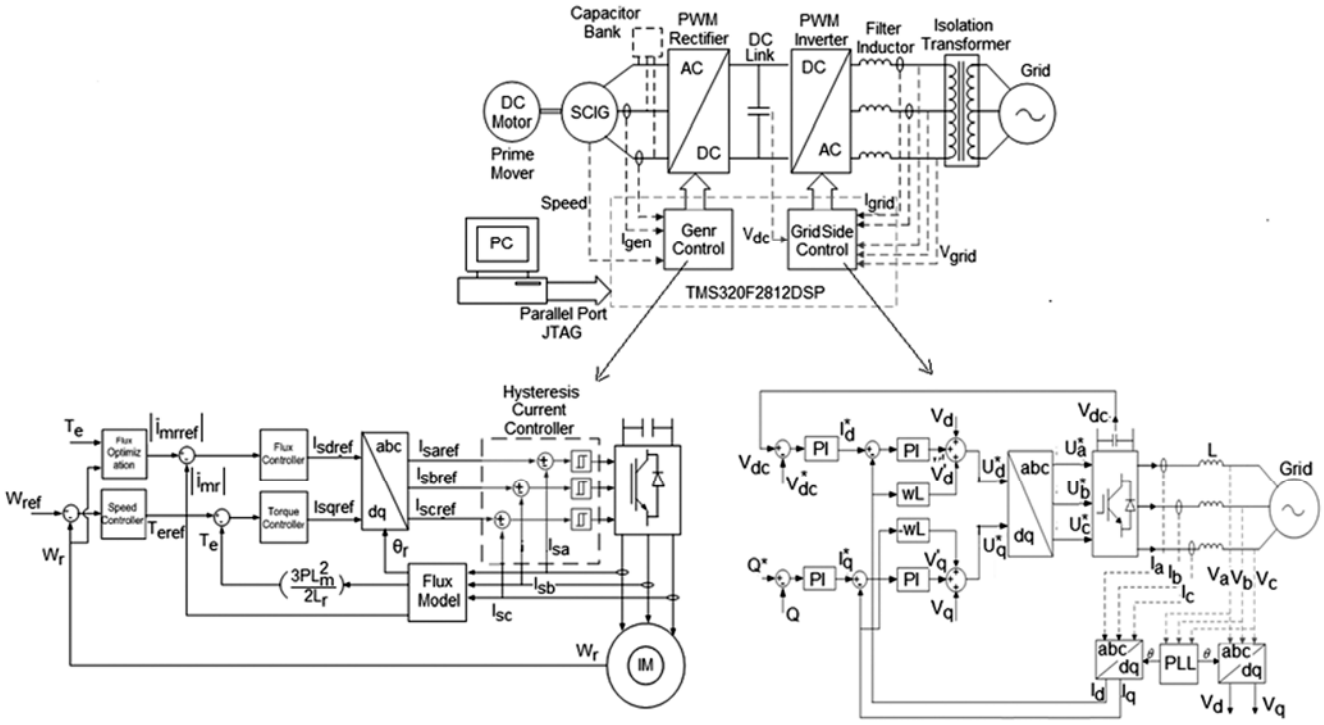

Fig. 1 — Schematic diagram for implementing SCIG based WECS with back to back VSCs and the internal control schemes for the machine side and the grid side control

controllers provide the voltage reference for the converter which is compensated by adding the rotational EMF terms. To improve the performance of PI controller, cross-coupling strategy and voltage feed-forward control are used. The parameters of the PI controllers for inner current control loop and outer voltage control loop are tuned by using modulus optimum and symmetry optimum techniques respectively. The phase angle needed by the abc - dq conversion module is obtained from the grid voltages using a phase locked loop. The interface reactance 'L' filters high frequency ripple in the voltages due to the switching of the converter devices.

Experimental Results

The following section discuss the dynamic behavior of the SCIG based WECS based on the total energy extracted, power quality at the grid interface point and the range of wind speed that can be handled. MPPT algorithm based on vector control technique is used for the MSC and so, the generator speed tracks the wind speed variations so that optimum tip speed ratio is maintained. The generator current, grid current and generated power varies proportionally with the wind speed. The hardware results for back to back connected converter based WECS using SCIG is shown in Fig. 2. One can observe proportional variation in grid current and generator current, which depicts a proportional variation in output power and hence the ability to track maximum power point. DC link voltage remains constant for all power fluctuations, which shows the ability of the system to respond to sudden wind velocity variations. It can be clearly seen that the generator and GSC currents vary as per the variations in the speed.

This section also brings out the results on power quality aspects relating to the said control. The results obtained for generated voltages and currents of the induction generator having PWM converter at machine terminals, for 800 rpm and 1200 rpm are illustrated in Fig. 2. There is no additional reactance intervening between the MSC and the machine and hence the switching voltages of the MSC are clearly seen at the machine terminals. However, the currents are fairly sinusoidal. One of the concerns of connecting WT to the grid is power quality, as the wind energy provides an unpredictable and fluctuating power. Use of power electronics converters is the another major reason for introducing harmonics to the grid.[10]

The voltage and current waveforms at the output terminals of the GSC, for a generator speed of 1200 rpm is shown in Fig. 3 — a fairly sinusoidal voltage

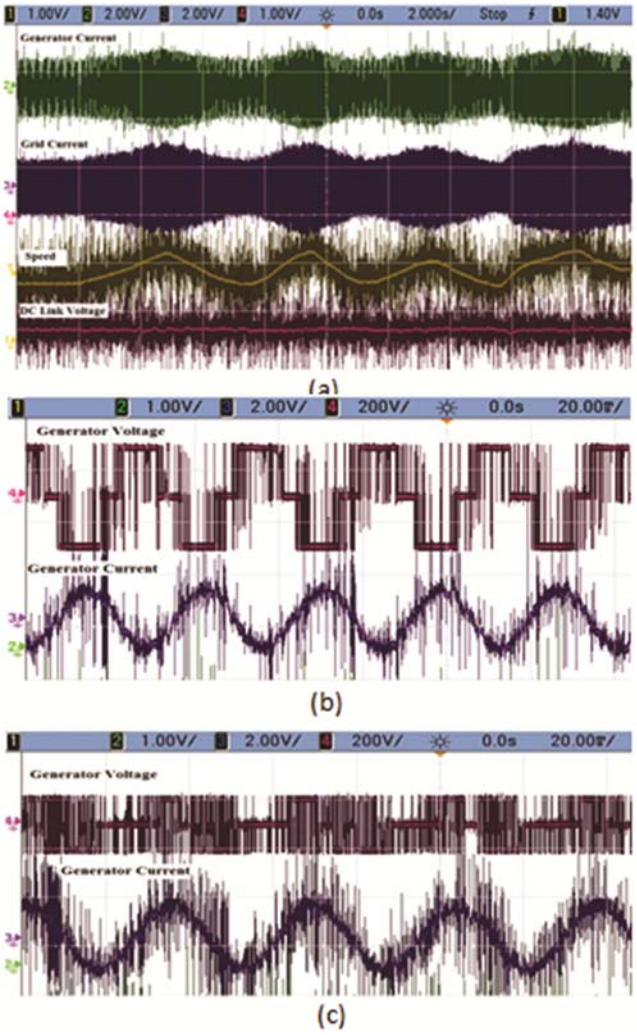

Fig. 2 — Hardware results for (a) WECS - speed variation from 800 to 1200 rpm (b and c) Generated voltages and currents at 800 rpm and 1200 rpm generator speed

and current at the GSC terminals resulting in less than 10% THD as depicted in the next two snap-shots (Fig. 3(a)); the THD of the voltage is 9.6% (Fig 3(b)); a THD of 5.3% for the current waveform (Fig. 3(c)). The resulting waveforms for voltage and current at the output terminals of the step-up transformer, connected between the GSC and grid, are also shown in the same Fig. 3 — the actual grid voltage after the transformer, where the THD of voltage is only 1.5% are shown in Figs 3 (d) and (e). To satisfy the grid code requirements for the WECS, this THD is well in bounds. The Displacement Power Factor (DPF) of the grid side converter is again observed to be 1, which assures that a minimum converter rating can be adopted for this application.

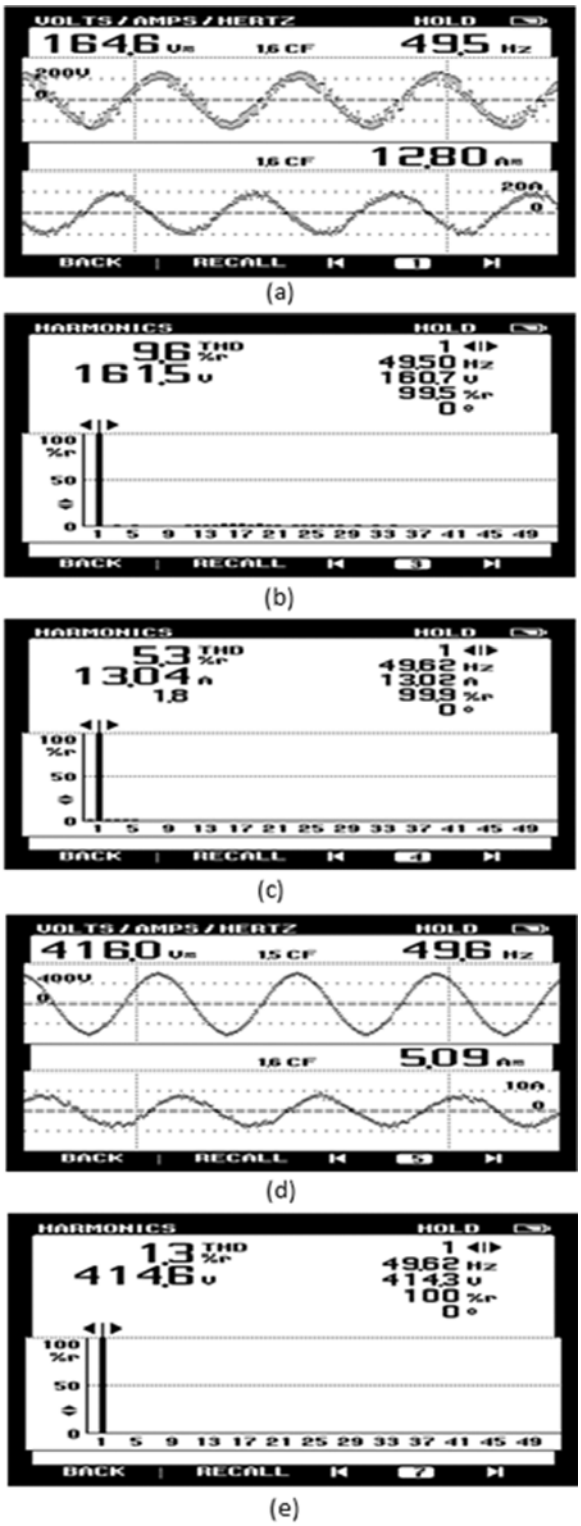

Fig. 3 — Hardware results for SCIG based WECS (a) Voltages and currents at GSC terminals (b) THD for voltage at GSC (c) THD for output current through GSC (d) Voltages and currents at the output terminals of the step-up transformer and (e) voltage THD at the grid

Conclusion

This work presents engineering and design of an SCIG based variable speed WECS, with the help of hardware implementation. Through analysis on results, it is found that the system is able to respond to maximum range of wind speed delivering the best possible amount of output power along with an acceptable power quality. The system has been implemented in real time with a squirrel cage induction generator of 2.2 kW rating that is coupled to a dc drive that emulates the wind turbine behavior. A Texas Instrument DSP TMS320F2812 has been used for the control of both MSC and GSC. The code generation for the control is done from MATLAB simulink with the help of Target support package for C2000 series TI processors. Experimental results show the excellent dynamic response of the system. The power quality of the grid currents and voltages are found to be well within IEEE power quality standards. The work may further be extended to study the dynamic behavior under symmetrical and unsymmetrical fault conditions.

Acknowledgement

The research paper was created with the grant support by Dr A P J Abdul Kalam Technical University, Lucknow, Uttar Pradesh under the Collaborative Research and Innovation Program (CRIP). Authors are grateful to all those who contributed during this project.

References

1 Ahuja H & Kumar P, A novel approach for coordinated operation of variable speed wind energy conversion in smart grid applications, *Elsevier Comp & Elec Eng*, **77** (2019) 72–87.

2 Konstantopoulos G C & Alexandridis A T, Full-Scale Modeling, Control, and Analysis of Grid-Connected Wind Turbine Induction Generators with Back-to-Back AC/DC/AC Converters, *IEEE Journal of Emerging and Selected Topics in Power Electronics*, **2(4)** (2014) 739–748.

3 Simani S, Overview of Modelling and Advanced Control Strategies for Wind Turbine Systems, **8** (2015) 13395–13418.

4 Tripathi S M, Tiwari A N & Singh D, Grid-integrated permanent magnet synchronous generator based wind energy conversion systems: A technology review, *Renew & Sust Ener Reviews*, **51** (2015) 1288–1305.

5 Ahuja H, Sharma S, Singh G, Sharma A & Singh A, Coordinated Fault Ride Through Strategy for SCIG based WECS, *2nd IEEE conf on comp intelligence and comm tech*, (2016) 1–6.

6 Bose B K & Wang F, Power Electronics in renewable Energy Systems and Smart Grid. John Wiley & Sons Inc., Hoboken, New Jersey, (2019) 14–51.

7 Yaramasu V, Wu B, Sen P C, Kouro S & Narimani M, High-power wind energy conversion systems: State-of-the-art and emerging technologies, *Proceedings of the IEEE,* **103(5)** (2015) 740–788.

8 Ahuja H, Virmani R & Ahuja A, Performance comparison of most prevalent wind energy conversion systems, *7th India Int Conf on Power Electronics* (2016) 1–6.

9 V Meenakshi & S Paramasivam, Design of LCL Filter in Front End Converters Suitable for Grid Connected Wind Electric Generators, *J Sci Ind Res*, **78** (2019) 896–899.

10 N Archana & R Vidhyapriya, A Novel SRF Based UPFC in Grid Connected Wind and Solar Hybrid System, *J Sci Ind Res*, **75** (2016) 720–724.